Axons provide the secretory machinery for trafficking of voltage-gated sodium channels in peripheral nerve

Carolina González[a,b], José Cánovas[a,b], Javiera Fresno[a,b], Eduardo Couve[c], Felipe A. Court[d], and Andrés Couve[a,b,1]

[a]Program of Physiology and Biophysics, Institute of Biomedical Sciences, Faculty of Medicine, Universidad de Chile, 8380453 Santiago, Chile; [b]Biomedical Neuroscience Institute, Faculty of Medicine, Universidad de Chile, 8380453 Santiago, Chile; [c]Instituto de Biología, Laboratorio de Microscopía Electrónica, Facultad de Ciencias, Universidad de Valparaíso, 2360102 Valparaíso, Chile; and [d]Faculty of Biological Sciences, Pontificia Universidad Católica de Chile, 8331150 Santiago, Chile

Edited by William A. Catterall, University of Washington School of Medicine, Seattle, WA, and approved January 8, 2016 (received for review July 29, 2015)

The regulation of the axonal proteome is key to generate and maintain neural function. Fast and slow axoplasmic waves have been known for decades, but alternative mechanisms to control the abundance of axonal proteins based on local synthesis have also been identified. The presence of the endoplasmic reticulum has been documented in peripheral axons, but it is still unknown whether this localized organelle participates in the delivery of axonal membrane proteins. Voltage-gated sodium channels are responsible for action potentials and are mostly concentrated in the axon initial segment and nodes of Ranvier. Despite their fundamental role, little is known about the intracellular trafficking mechanisms that govern their availability in mature axons. Here we describe the secretory machinery in axons and its contribution to plasma membrane delivery of sodium channels. The distribution of axonal secretory components was evaluated in axons of the sciatic nerve and in spinal nerve axons after in vivo electroporation. Intracellular protein trafficking was pharmacologically blocked in vivo and in vitro. Axonal voltage-gated sodium channel mRNA and local trafficking were examined by RT-PCR and a retention-release methodology. We demonstrate that mature axons contain components of the endoplasmic reticulum and other biosynthetic organelles. Axonal organelles and sodium channel localization are sensitive to local blockade of the endoplasmic reticulum to Golgi transport. More importantly, secretory organelles are capable of delivering sodium channels to the plasma membrane in isolated axons, demonstrating an intrinsic capacity of the axonal biosynthetic route in regulating the axonal proteome in mammalian axons.

axon | endoplasmic reticulum | trafficking

Neurons are among the largest and most complex eukaryotic cells. Although they differ in size and shape, most neurons are polarized in axonal and somatodendritic compartments. The establishment and maintenance of neuronal polarity, the rate and directionality of axonal growth, synapse formation, and plasticity are determined by the axonal proteome (1).

Fast and slow axonal transport govern the availability of axonal components through anterograde and retrograde fluxes (2). However, energetic and temporal considerations suggest that transport may not be sufficient to control the immediate requirements of the distal proteome, especially under conditions of regeneration (3). Localization of mRNA and de novo protein synthesis provide an alternative to respond quickly to local demands (4).

Local biosynthesis and processing are supported by the identification of ribosomes in immature and mature peripheral and central nervous system axons (5–7). They are sustained, in addition, by the identification of hundreds of axonal mRNAs localized in axons of the squid, *Aplysia*, *Xenopus*, and mammals (8). Direct evidence of axonal translation in several vertebrate and invertebrate models also back this claim (9, 10). Indeed, local protein synthesis plays an important role in axonal development and maintenance and occurs in response to internal and external cues (11–14). These studies have focused on the identification of mRNAs and the synthesis of cytosolic proteins. However, the transcriptome is by no means limited to soluble proteins.

Local biosynthesis of membrane proteins requires functional processing stations including the endoplasmic reticulum (ER), the intermediate compartment between the ER and the Golgi apparatus (ERGIC), and the Golgi (1). Multiple components of the secretory route have been described in axons supporting the idea of an axonal secretory pathway (15–20). Isolated invertebrate axons are capable of synthesizing and inserting a plasma membrane G protein-coupled receptor after direct axonal injection of mRNA (21), and severed chick axons supply the plasma membrane with de novo synthesized EphA2 receptors (22). However, definitive proof of an axonal route for membrane proteins has not been adequately provided in mammalian neurons. Likewise, despite widespread knowledge on assembly and maintenance of nodal components (23), and on the clustering and anchoring of voltage-gated sodium channels (NaVs) at nodes of Ranvier (24–26), the trafficking mechanisms governing their surface delivery remains a mystery.

In the present study, we hypothesize that trafficking through the axonal ER is necessary for delivery of NaVs in peripheral neurons. We analyzed the distribution of endogenous and recombinant secretory pathway components by electron microscopy (EM), confocal microscopy, and in vivo electroporation. We explored the ER export capacity of the axon using pharmacological blockade of ER-Golgi trafficking and evaluated the presence of NaV mRNA by RT-PCR in rat sciatic nerve and cultures of dorsal root ganglia (DRG) neurons. Importantly, we used loss and gain of function approaches in vivo and in DRG cultures to examine the axonal trafficking and delivery of NaVs in peripheral axons.

Significance

Regulation of the axonal protein content is fundamental to maintain neural function. The transport of ready-made proteins by fast and slow mechanisms has been extensively studied, but local synthesis may also define the composition of the axon, in particular during adaptation or recovery. Accumulated evidence suggests that a proportion of cytosolic proteins are locally translated, but very little is known about membrane proteins. Our findings show the distribution of the endoplasmic reticulum and secretory organelles in peripheral axons and demonstrate for the first time, to our knowledge, an autonomous capacity of the axonal biosynthetic system in delivering membrane proteins, namely sodium channels, to the plasma membrane. These results contribute to our understanding of axonal trafficking and may be relevant for axonal regeneration.

Author contributions: C.G., F.A.C., and A.C. designed research; C.G., J.C., J.F., E.C., F.A.C., and A.C. performed research; E.C. and F.A.C. contributed new reagents/analytic tools; C.G., J.C., and J.F. analyzed data; and C.G., J.C., and A.C. wrote the paper.

The authors declare no conflict of interest.

This article is a PNAS Direct Submission.

[1]To whom correspondence should be addressed. Email: andres@neuro.med.uchile.cl.

This article contains supporting information online at www.pnas.org/lookup/suppl/doi:10.1073/pnas.1514943113/-/DCSupplemental.

Results

Localization of Early Secretory Organelles in Peripheral Axons. To address whether an axonal or local trafficking route participates in the delivery of NaVs, we initially determined the presence of biosynthetic components in axons of the rat sciatic nerve. We first examined the distribution of intracellular membranes by EM. Abundant mitochondria and a variety of membranous organelles were observed along the axon, with prominent ER tubular profiles that packed densely and anastomosed into irregular vesicle and beaded-like structures near the node (Fig. 1*A* and Fig. S1). We then explored the distribution of the biosynthetic machinery by immunofluorescence and confocal microscopy. We used antibodies that identify molecular determinants, resident enzymes, or structural components of secretory organelles (Fig. S2). Neurofilament staining precisely circumscribed the axonal shaft, and nodal regions were distinguished by the characteristic constriction of the neurofilament pattern (Fig. 1*B*). Constrictions correlated with nodes of Ranvier, identified by the enrichment of NaVs, and paranodal sections identified by contactin-associated protein (CASPR) (Fig. 1*B*). For subsequent analyses nodes were identified morphologically. Longitudinal, midsegment optical planes of myelinated axons revealed discrete ER-related structures in nodal and internodal regions (Fig. 1*C*, KDEL and ERP72). Magnified and rotated 3D reconstructions of nodal and internodal segments confirmed the presence of these markers in the axonal shaft. Notably, Sec23, a component of the COPII export machinery (27), was also observed in the axon. The ERGIC has not been thoroughly characterized in axons. Staining with pERGIC-53/p58 antibodies revealed a punctate profile within the axon especially in the internodal region (Fig. 1*C*, ERGIC). Golgi and trans-Golgi network (TGN) antibodies identified discrete structures in the axoplasm of nodal and internodal regions (Fig. 1*C*, Giantin and TGN46). We measured the intensity of endogenous secretory components along a longitudinally invariable region whose center was placed on the node of Ranvier identified by the paranodal marker CASPR. Moderate peaks of enrichment were observed for ER components at the node, whereas ERGIC and Golgi components were highly concentrated at the nodal or paranodal sections (Fig. 1*D*). Prominent peripheral nodal staining of ERGIC and, to a lesser degree, TGN46 suggests that these components may also be enriched in Schwann cells (Fig. 1*C*).

The distribution of components of biosynthetic organelles in myelinated axons suggests that nodal and internodal regions contain the machinery for secretory trafficking. To provide conclusive evidence that these components are localized to the axoplasm and exclude a potential glial source, we implemented in vivo electroporation of fluorescent reporters in adult rat DRG (Fig. 2*A* and Fig. S3). Electroporated ER retention signal (KDEL)-red fluorescent protein (RFP), translocon component (SEC61)-blue fluorescent protein (BFP), ERGIC-yellow fluorescent protein (YFP), and Golgi-YFP were synthesized and transported to axons (Fig. 2*B*). Expression of these reporter proteins was abundant both in the internodal and nodal regions, and all of them were enriched at the node (Fig. 2*C*). KDEL and SEC61 concentrated moderately, whereas ERGIC and Golgi components were highly enriched. To determine whether a topological relationship exists between different organelles, KDEL-RFP and Golgi-YFP were coelectroporated. These reporters partially colocalized indicating that ER and Golgi components are intimately associated at the node (Fig. 2*D*, arrows). Thus, secretory components localize to the distal axoplasm and appear to accumulate differentially at the node of Ranvier.

ER to Golgi Trafficking in Axons. Next we examined whether ER to Golgi transport operates locally in axons both in vivo and in vitro. To this end, we used pharmacological blockade of ER-Golgi transport using brefeldin-A (BFA), an inhibitor of COPI formation, and the related, but *cis*-Golgi specific, Golgicide-A (GCA). Treatment with these drugs results in disassembly of the Golgi complex and accumulation of cargo in the ER (Fig. S4) (28, 29). ER to Golgi transport occurring in the axon should display sensitivity to these drugs when applied locally, i.e., far from the neuronal soma, whereas conventional motor-mediated transport of post-Golgi vesicles should be unaffected. We first injected BFA in the distal sciatic nerve of the rat and evaluated the abundance of membranous organelles in the nodal axoplasm by EM. Numerous heterogeneous membranes were observed in the axoplasm, particularly in the nodal region of large caliber axons (Fig. 3*A*, *Left*). A marked decrease in membranous organelles in the nodal region was observed after exposure to BFA, despite the fact that the overall organization of the node, compact myelin and the paranodal loops were unaffected (Fig. 3*A*, *Right*). A

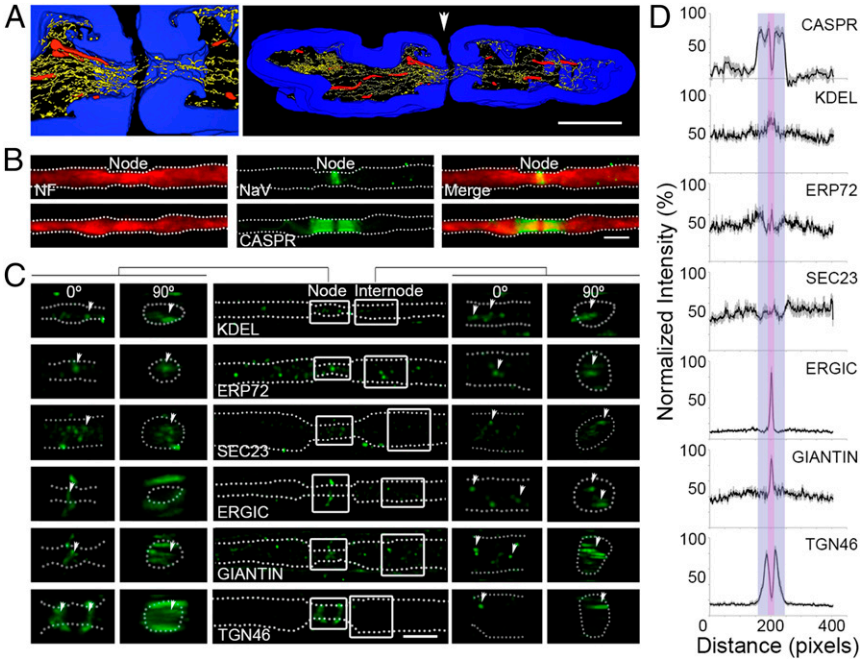

Fig. 1. Endogenous secretory components in myelinated axons. (*A*) 3D EM reconstruction of intracellular membranes at the node of Ranvier (arrowhead) and adjacent regions. ER network (yellow), mitochondria (red), and myelin sheath (blue). (*Left*) Magnification of the nodal region. (*B*) Epifluorescent images of sciatic nerve dissociated axons. Neurofilament (NF), NaV, and CASPR. (*C*) Nodal and internodal z-stack projections showing the distribution of the ER markers KDEL and ERP72, the COPII ER export component SEC23, the ERGIC marker p58, and the Golgi markers Giantin and TGN-46. NF was used to define the axonal outline (dashed line). Magnifications of nodes (*Left*) and internodes (*Right*) without or with rotation (0° and 90°, respectively). Axons are representative of at least three independent experiments. (*D*) Distribution analysis of the secretory markers in nodes and internodes shown in *C*. Intensity of each pixel was measured along a region of interest of 404 × 61 pixels (35.5 × 5.4 μm) centered at the node (pink) identified by CASPR (purple). The average intensity of seven to eight axons was plotted. (Scale bars, 5 μm.)

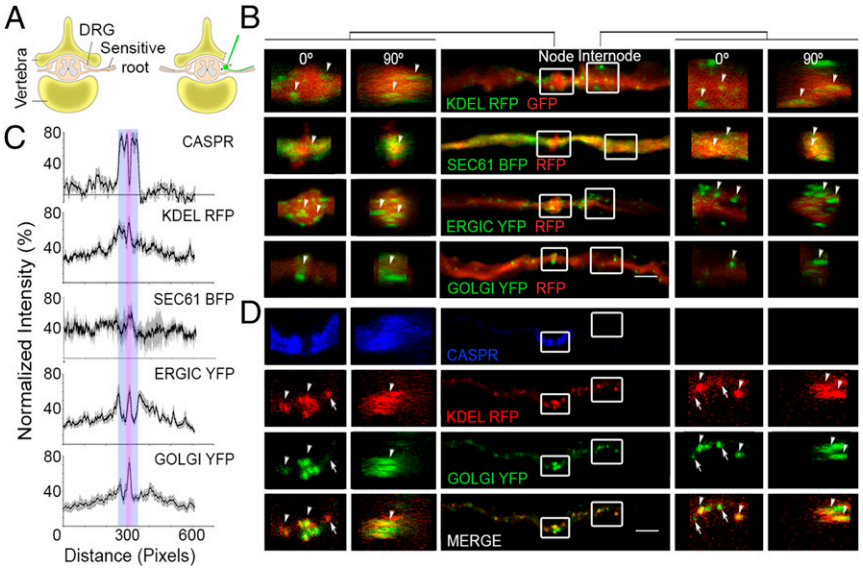

Fig. 2. Exogenous secretory components in myelinated axons. (*A*) Diagram of in vivo DRG electroporation. L4 or L5 DRGs were exposed and electroporated. (*B*) Expression of the secretory markers KDEL-RFP, SEC61-BFP, ERGIC-YFP, and Golgi-YFP in axons of the spinal nerve after in vivo DRG electroporation. All markers were coelectroporated with soluble GFP or RFP. (*C*) Distribution analysis of the secretory markers in nodes of Ranvier and internodes shown in *B*. Intensity of each pixel was measured along a region of interest of 611 × 108 pixels (83.7 × 14.8 μm) centered at the node (pink) identified by CASPR (purple). The average intensity of 5–15 axons was plotted. (*D*) In vivo DRG coelectroporation of KDEL and Golgi markers. Magnifications of nodes (*Left*) and internodes (*Right*) without or with rotation (0° and 90°, respectively). (Scale bars, 5 μm.) Axons are representative of at least three independent experiments.

drastic decrease of membranous organelles and the appearance of a prominent ER network in the cytoplasm of fibroblasts from the same portion of sciatic nerve confirmed the characteristic effect of BFA (Fig. 3*A*, *Lower*). These observations suggest a local ER-Golgi mode of transport in the axon.

In these experiments, axonal organelles may be indirectly affected by glial dysfunction as a result of BFA treatment. To evaluate the effect of local ER to Golgi blockade nonambiguously, we established an in vitro model in Boyden chambers consisting of a purified axonal preparation from DRG neurons cultured on a 3-μm porous substrate that allows selective elimination of the somatic or axonal domains (Fig. 3*B*). Desomatized DRG axons were treated with BFA or GCA for 60 min, and discrete ER and TGN structures were measured. As expected for local ER-Golgi transport, a significant increase in the number of TGN particles were observed in isolated axons after BFA and GCA treatments, whereas the number of ER particles remained unchanged (Fig. 3 *C* and *D*). Neurofilament staining showed no signs of fragmentation in our experimental setup, indicating that axons remain viable (Fig. S5). Taken together, these results demonstrate that COPI-dependent ER-Golgi trafficking in axons operates autonomously from the neuronal soma.

The Axonal ER Contributes to the Delivery of NaVs. Having revealed an axonal secretory machinery, we next sought to explore its contribution to the intracellular trafficking and delivery of NaVs. Because axonal translation is well established, we first determined whether NaVs were appropriate candidates for local processing. Sodium channel mRNAs have been identified in axons of sensory neurons (30). However, to our knowledge, NaV1.2, NaV1.6, or β2-NaV mRNAs have not been reported. We thus examined the presence of their transcripts in axons by RT-PCR. We designed primers for NaVs (NaV1.6, NaV1.2, PanNaV, and β2-NaV), the axonal protein neurofilament (NF), the myelin protein P0, the somato-dendritic marker MAP2, and β-actin. As expected, samples from the sciatic nerve did not contain detectable levels of NaV1.2, expressed only in immature axons, or MAP2, in agreement with its somato-dendritic distribution. More importantly, NaV1.6 and β2-NaV were expressed in the sciatic nerve in agreement with their expression in mature axons (Fig. 4*A*, *Upper*) (31). P0 was also detected in these samples indicating that Schwann cell material is part of the preparation and therefore that it cannot be used to nonambiguously define axonal transcripts. To circumvent these limitations we repeated the procedure in DRG cultures where all transcripts, except NaV1.2, were identified (Fig. 4*A*, *Lower*). To eliminate somatic transcripts we again used an isolated axonal system of desomatized embryonic DRG explants. After desomatization, DRG explants did not contain nuclear or somato-dendritic markers (Fig. S6). Interestingly, NaV transcripts were expressed in these purified axonal samples (Fig. 4*B*). In addition, a replacement from NaV1.2 to NaV1.6 was observed in DRG explants desomatized after 6 or 14 d in vitro (div) in agreement with the known transition of these channel isoforms in developing nodes (32). The somato-dendritic and Schwann cell markers were absent confirming the purity of the axonal preparation. These observations demonstrate that the transcript for NaV1.6 is present in DRG axons and, admitting that local biosynthesis has not been shown directly, they prompted us to use NaVs as cargo model to center on axonal secretory trafficking.

We first explored whether the axonal secretory machinery is necessary for delivering NaVs to the nodal plasma membrane in vivo. NaVs were abundant at nodes of Ranvier of dissected axons, showing a characteristic ring-like pattern, indicative of their enrichment at the cell surface (Fig. 4*C*, Control). Twenty-four hours after injection of BFA at the distal sciatic nerve, they redistributed toward the nodal axoplasm and filled the ring-like profile (Fig. 4*C*, BFA). Measurements of the intensity signals along transects at the node in control conditions revealed two peaks corresponding to the concentration of the NaVs in the nodal membrane and a depression corresponding to the nodal axoplasm (Fig. 4*C*, *Right,* red curve). In the presence of BFA, there was a significant reduction in the depression, indicating redistribution of NaVs in the axoplasmic region (Fig. 4*C*, *Right*, blue curve). Similar results were obtained with GCA (Fig. S7). Discrete NaV-containing structures also appeared along the axonal internode after BFA or GCA treatment, indicating that the effect was not restricted to the nodal region (Fig. 4*D* and Fig. S7). Importantly, the distribution of neurofilament was unaltered, discarding a nonspecific effect on axonal proteins (Fig. S7). These results indicate that local blockade of COPI-dependent ER-Golgi transport results in the redistribution of NaVs in intracellular compartments, most likely the ER. They support local axonal ER trafficking of NaVs, without discarding the contribution of transport-based mechanisms.

Finally we set out to demonstrate whether the axonal trafficking machinery is sufficient to deliver NaVs to the cell surface. We took advantage of a recently developed strategy to retain reporter proteins in the ER and release them synchronously after addition of a rapamycin analog [DD-solubilizer (DD)] (33). We used the single transmembrane domain β2 subunit of the NaV, which is bound to the α subunit via disulfide bonds and assembles into the

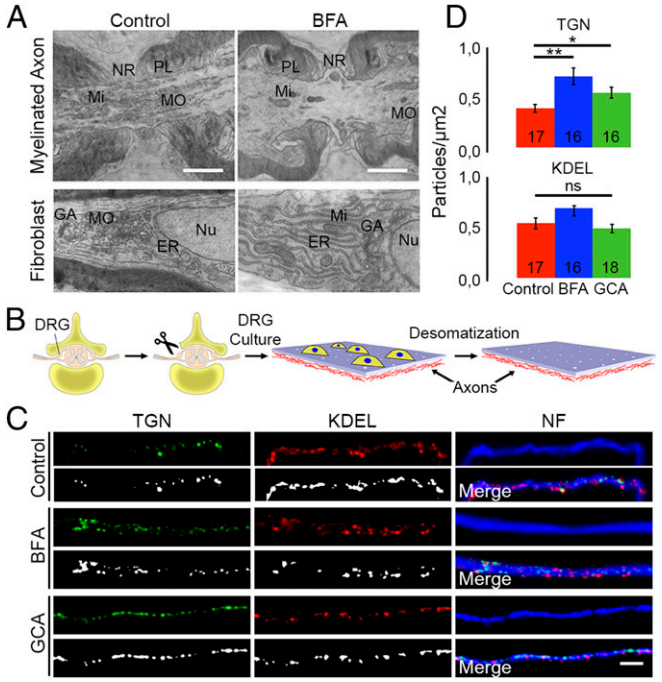

Fig. 3. ER-Golgi trafficking in peripheral axons. (*A*) Transmission EM of axons and fibroblasts in control (*Left*) or BFA-treated sciatic nerves (*Right*). NR, nodes of Ranvier; PL, paranodal loops; Mi, mitochondria; MO, membranous organelles; Nu, nucleus; GA, Golgi apparatus; ER, endoplasmic reticulum. (Scale bar, 1 μM.) Results are representative of three independent experiments. (*B*) Schematic representation of the protocol used for isolation of DRG axons. Cell bodies and nonneuronal cells remained on the upper surface. Isolated axons were obtained by scraping the upper surface. (*C*) Effect of BFA (*Middle*) and GCA (*Bottom*) in the distribution Golgi marker TGN (green), the ER marker KDEL (red) and neurofilament (blue) in isolated axons. Segmentation used for analysis (black and white) is shown below each panel. (Scale bar, 3 μm.) (*D*) Quantification of TGN and KDEL particles in control and BFA- and GCA-treated axons. $*P < 0.05$; $**P < 0.005$; ns, nonsignificant; Student *t* test.

NaV complex before insertion into the nodal membrane thus constituting a good trafficking reporter amenable to molecular manipulation and transfection (34). We generated an FM4-β2-GFP fusion protein composed of four FM domains, a myc epitope, the transmembrane β2 subunit, and GFP. The FM domains and myc epitope are exposed to the ER lumen/extracellular milieu, whereas GFP is cytosolic (Fig. 4*E*). This design allows ER retention of the reporter protein due to FM domain aggregation and subsequent pharmacological release by DD for Golgi processing and membrane insertion, exposing the MYC epitope to the extracellular compartment (Fig. 4*F*). Following nucleofection in nonneuronal cells, FM4-β2-GFP was effectively retained in the ER and released by DD becoming enriched at the plasma membrane after 90 min (Fig. S8*A*). In whole cultures of DRG neurons, FM4-β2-GFP expressed for 20 h was also retained in the ER and was delivered to the plasma membrane on release (Fig. S8*A*). Importantly, DD resulted in a membrane distribution of FM4-β2-GFP in the soma and throughout the axonal length as indicated by neurofilament staining (Fig. 4*G*). Crucially, if ER release was elicited after the somas were removed, FM4-β2-GFP was delivered to the axonal plasma membrane in isolated axons (Fig. 4*H*). FM4-β2-GFP trafficked efficiently to the plasma membrane after incubation with DD (0/21 axons, 0%, control conditions; 15/20 axons, 75%, DD; $n = 6$ independent experiments, $P < 0.0001$ χ^2 test). We also noted surface FM4-β2-GFP in neurofilament-negative cellular projections after DD (Fig. S8*B*; 0/10 projections, 0%, control conditions; 12/15 projections, 80%; $n = 6$ independent experiments, $P = 0.0001$, χ^2 test) indicating that local trafficking also takes place in nonneuronal cells. These observations provide direct evidence that FM4-β2-GFP retained in the axonal ER is exported and delivered to the plasma membrane locally, independently of the neuronal cell body in vitro.

Discussion

Combined, our experiments provide the first direct demonstration, to our knowledge, of ER to cell surface delivery of membrane proteins in mammalian axons. They show that early secretory components localize to the distal axoplasm and that, on overexpression, are enriched at nodes of Ranvier. They also indicate that an ER to Golgi trafficking route operates in axons, revealing an early biosynthetic machinery capable of locally processing membrane proteins. Additionally, they provide evidence to support a role for axonal secretory organelles in the local trafficking of sodium channels. Indeed, our results demonstrate that the transcripts for NaV1.6 are localized to the axon, and critically, that sodium channel subunits are retained in the axonal ER, and exported locally to the plasma membrane independently of the neuronal cell body.

The distribution of organelle components in axons of the sciatic nerve and DRG cultures and the sensitivity of intracellular membranes and NaV distribution to local BFA and GCA indicate that a functional secretory machinery operates in axons. Previously, the axonal ER has been described as a continuous 3D interconnected network, associating many resident and functional components. Tubule-vesicular structures, different from those found in the internodal areas, have been reported at the nodes of Ranvier (17), and COPII export sites containing Sar1 promote axonal growth in culture (35). Specific markers for ERGIC and Golgi have also been described in central and peripheral axons and may contribute to axonal function (36). Our findings fully support these earlier observations, but in addition provide functional evidence of COPI activity in the axon.

A marked enrichment of secretory route components at nodes of Ranvier was visible using expression of fluorescent reporters. Whether overexpression contributes to this exquisite distribution remains to be explored. However, the differential enrichment of KDEL-RFP, SEC61-BFP, and Golgi-YFP at the nodes strongly argues against a nonspecific aggregation phenomena caused by the nodal constriction. In addition, the preferential distribution of ERGIC-YFP at the node and its symmetric accumulation at the boundaries of the paranodes indicate that individual patterns are highly specific and unique for different secretory components.

What signals target these components to axons and possibly to axonal microdomains remains unknown. Furthermore, whether these structures represent morphologically identifiable organelles or transient structures with mixed identities requires closer examination. Additional experiments are also needed to determine whether secretory stations are highly localized at nodes of Ranvier or if they are prominent throughout the axoplasm in vivo and if differences exist between myelinated and nonmyelinated axons. Membranous organelles along axonal shafts and in nodes have been observed previously by EM (17, 18). However, EM is unsuitable for characterizing their molecular composition and origin. New superresolution microscopy, which provides the spatial range suitable for visualizing the narrow axonal shaft, represents an attractive and feasible avenue to explore the molecular composition of secretory membranes along the axon. Intriguingly, precise nodal and paranodal distributions that were excluded from the neurofilament boundary were consistently observed for endogenous ERGIC and TGN, suggesting that Schwann cells also localize early secretory machinery. Despite these considerations, the present study demonstrates that the mammalian axon constitutes an autonomous trafficking domain.

Myelinated axons are organized in polarized domains around nodes of Ranvier, which are characterized by a high density of α and β NaVs (24). NaV1.6 is specific to mature nodes, whereas NaV1.2 is expressed primarily in nonmyelinated axons, specifically in the axon initial segment and immature nodes (32). β accessory subunits regulate trafficking, kinetics, voltage dependence, and localization of NaVs at nodes of Ranvier and the axon initial segment (37). NaVs are stabilized by both binding to ankyrin-G

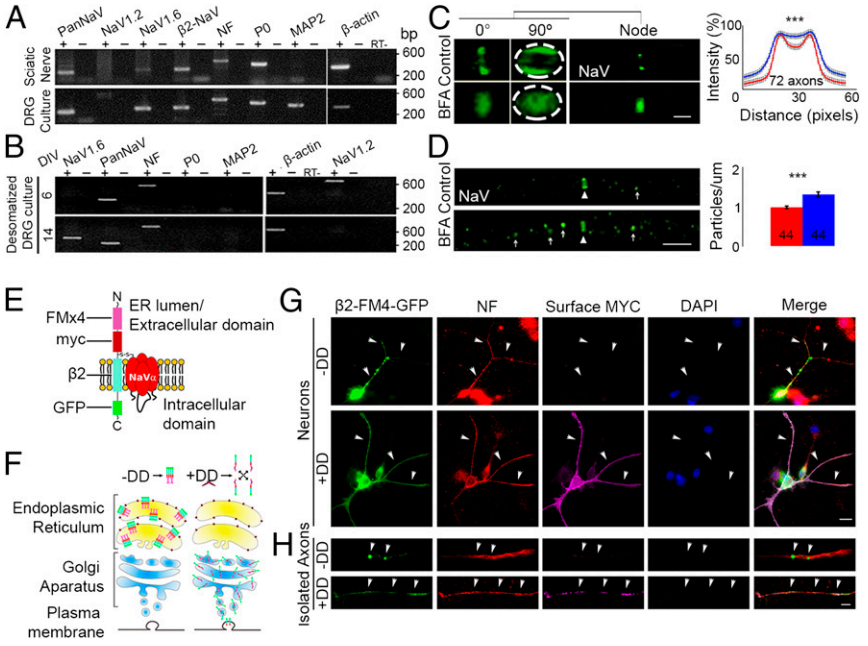

Fig. 4. Axonal trafficking of voltage-gated sodium channels in vivo and in vitro. (*A* and *B*) RT-PCR in samples derived from adult rat sciatic nerve and embryonic DRG cultures of 14 div and from DRG explants desomatized after 6 or 14 div. Reaction with (+) or without (–) cDNA. Retrotranscriptase reaction without enzyme (RT–). (*C*) Distribution of NaV in nodes of Ranvier of dissociated axons from sciatic nerves injected in vivo with vehicle (control) or BFA. Magnifications without or with rotation (0° and 90°, respectively; *Left*). (*Right*) Intensity of each pixel along a region of interest of 54 × 24 pixels (5.4 × 2.4 μm) centered vertically at nodes of Ranvier was measured and plotted in control or BFA-treated nerves. (*D*) Distribution of NaVs in axons of sciatic nerves treated in *C*. NaV signal at nodes (arrowheads) and outside (arrows). (*Right*) Number of NaV puncta in control or BFA were measured and plotted. ***$P < 0.0001$, Student *t* test. (*E*) Diagram of the β2 subunit construct coupled with the FM4 domains (FM4-β2-GFP). (*F*) In the absence of DD, the FM4 domains are aggregated and retained in the ER. After incubation with DD, FM4-β2-GFP is delivered to the plasma membrane. (*G*) Dissociated DRG neurons were transfected with FM4-β2-GFP. Twenty hours after transfection, cells were treated (+) or not (–) with DD. Surface expression was detected with anti-myc antibodies in live cells. (*H*) Dissociated DRG cells were transfected as in *G*. Cells were desomatized and isolated axons were treated (+) or not (–) with DD. Axons were identified by neurofilament (NF) staining. [Scale bars, 2 μm (*C*); 5 μm (*D*, *G*, and *H*).] All results are representative of three independent experiments.

and the paranodal loops that prevent lateral movement (38). Our data indicate that the transcript for NaV1.6 is localized to the axon. Fast axonal transport may contribute to localize the mRNA to distal axons. Alternatively, NaV1.6 mRNA may be transferred from Schwann cells through vesicular structures (39). However, the presence of mRNA in pure axons in cultured explants devoid of Schwann cells favor a transport model. A detailed characterization of the 5′ and 3′ UTR may provide insights into the mechanisms of transport and localization.

The relative contribution of transport and local trafficking for membrane protein delivery in the axon remain to be investigated in detail. In myelinating axons of cultured neurons, the adhesion molecules NF186 and NrCAM concentrate via lateral diffusion and "trapping" during node assembly, whereas NaVs rely on BFA-dependent vesicular transport (40). However, the mechanism of NaV delivery has not been evaluated in mature axons. Additionally, somatic BFA treatment does not discriminate between somatic synthesis/long-haul transport and local ER/plasma membrane trafficking. Other studies have identified a physical interaction between kinesin and NaV1.8, but not NaV1.6 (41). Whether this reflects a preference for a particular supply mechanism is not yet clear. In addition, the contribution of posttranslation modifications at the Golgi apparatus or other post-ER organelles remains to be studied. It is certainly possible to envision differential modifications in somatic and local organelles that may result in functional variability.

Local biosynthesis and trafficking may provide the means to rapidly regulate the axonal proteome in response to developmental requirements or structural plasticity or to ensure efficient repair after damage. Understanding how the local machineries respond to physiological or pathological demands may provide new insights into axonal function and organelle biogenesis and may provide new alternatives for control and intervention.

Materials and Methods

Antibodies, Chemicals, cDNAs, and Primers. The following antibodies were used: rabbit anti-KDEL and anti-ERP72 (Thermo Fisher; PA1-013 and PA1-007, respectively), rabbit anti-ERGIC-53/p58 and anti-MYC (Sigma; E1031 and C3956, respectively), rabbit anti-Giantin (Covance; PRB-114C), rabbit anti-SEC23 and anti-CASPR (Abcam; Ab50672 and Ab34151, respectively), sheep anti-TGN46 (Novus Biologicals; NB110-60520), mouse anti-MAP2A, 2B and chicken anti-Neurofilament (Millipore; MAB378 and AB5735, respectively), rabbit anti-TGN38 (AbD Serotec; AHP1597), rabbit anti–PAN-NaV channel (Alomone Labs; ASC-003), FITC (711-095-152 and 703-095-155), TRITC (711-025-152, 715-025-150), Cy5 (711-175-152 and 703-175-155), Cy3 (703-165-155), and Alexa 488 (713-545-003) conjugated secondary antibodies (Jackson Laboratory). The following chemicals were used: D/D solubilizer (Clontech; 635054), Brefeldin A and Golgicide (Sigma; B7651 and G0923, respectively), and DAPI (Thermo Fisher; 62248).

pEGFP-N1 (GFP), pDsRed-C1 (RFP), pEYFP-Golgi, pEYFP-ERGIC, and pDsRed2-ER (ER-RFP) were from Clontech. BFP-Sec61β has been described previously (42). To generate FM4-β2-GFP-MYC, four FM domains were fused to the N terminus of the β2 subunit of NaV (Genewiz). The amplicon was inserted into the FM4-GFP vector between 5′ XhoI and 3′ PstI sites. Primers are shown in Table S1.

Animals and Surgical Procedures. Sprague–Dawley male rats were purchased from the Central Animal Facility at Facultad de Medicina, Universidad de Chile, and euthanized according to National Institutes of Health and Comisión Nacional de Investigación Científica y Tecnológica (CONICYT) (Chile) guidelines. The experimental protocol was approved by the Institutional Bioethics Committee (Universidad de Chile, 1140617). For all surgical procedures, adult rats (150–300 g) were anesthetized with oxygen and isoflurane [2–3% (vol/vol)]. To reduce the inflammatory response, animals were s.c. injected with ketoprofen before surgery (0.05%). In vivo DRG electroporation was performed as previously described (43). DRG and corresponding spinal nerve (~8-mm fragments from the DRG) were extracted 4 d after surgery. Sciatic nerves were exposed and injected at the sciatic notch with 2 μL BFA (50 μg/mL) or GCA (100 μM). Methanol or dimethyl sulfoxide was used as controls for BFA or GCA on the contralateral side. Injected segments were extracted 24 h after the surgical procedure and processed for immunofluorescence or EM.

DRG Cultures, Isolation of Axons, and Nucleofection. Embryonic DRG cultures were obtained as previously described (44). Desomatization was carried out under visual inspection in 6 or 14 div cultures using a sterile p1000 pipette. Adult DRG cultures were obtained as previously described (45). Isolation of axons was performed as previously described (46). ER to Golgi transport in dissociated DRGs was blocked with BFA (5 μg/mL) or GCA (10 μM) in complete medium for 1 h at 37 °C and 5% CO_2 and processed for immunofluorescence. Electroporations were performed using 2 μg KDEL-RFP and FM4-β2-GFP-MYC for double transfections or 4 μg FM4-β2-GFP-MYC for single transfections. Samples were electroporated using the AMAXA Nucleofector Apparatus (Lonza) and the Rat DRG Neuron O-003 program, using the Basic Neuron SCN Nucleofector KIT (Lonza). Cells were plated onto six-well coverslips or culture insert membranes (3-μm-diameter pores) for 20 h at 37 °C and 5% CO_2. Selective elimination of the somatic or axonal domains was performed as

CELL BIOLOGY

previously described (16). Cells or isolated axons were incubated with 2.5 μM DD for 90 min in complete medium at 37 °C and 5% CO_2.

RNA Extractions and RT-PCR. Extractions of RNA from sciatic nerve and embryonic DRG cultures were achieved using Trizol. Extraction of RNA from embryonic axonal preparations was performed using RNAqueous-Micro Kit (Life Technologies). cDNA synthesis was performed using the SuperScriptIII First-Strand System using oligo-dT primers (Life Technologies). All subsequent PCR reactions were carried out using 2 μg cDNA and 35 cycles of amplification.

EM and Immunofluorescence. Anesthetized animals were perfused via the left ventricle with fixative solution containing 2.5% glutaraldehyde and 4% paraformaldehyde in 0.1 M sodium cacodylate buffer (pH 7.4). Sciatic nerves were removed, washed in cacodylate buffer, and postfixed for 2 h in reduced osmium (1% osmium tetroxide and 0.5% potassium ferrocyanide). Samples were dehydrated and embedded in epon resin (Embed-812; EMS). Ultrathin sections were mounted on grids, contrasted with uranyl acetate followed by lead citrate. Samples were observed and analyzed in a Zeiss EM900 transmission EM. For EM identification of ER and mitochondria, membranous structures were labeled manually, and those containing double membranes and morphological features of mitochondria (high electron density and presence of internal cristae) were assigned as mitochondria and colored in red. For ER, connected tubular structures were colored in yellow. Structures closely associated to tubular structures, including racemme-like groups, were also included in the yellow category. Due to the staining method, cytoskeletal structures with similar diameter (e.g., microtubules) were not heavily stained, and they do not interfere with the identification of membranous tubules.

Immunofluorescence for dissociated axons, embryonic DRG cultures and isolated axons, or adult DRG cultures were performed as previously described (46–48). We focused on large caliber axons, whose diameter ranged between 4 and 5 mm. Samples were observed and analyzed on a spectral confocal microscope Olympus FluoView FV1000 with a UPLSAPO 60×/1.35 objective, 3× digital zoom, KALMAN 3, and z longitudinal section of 0.2 μm (20–25 optical slices for each axon) or an Olympus BX61WI upright microscope with an UPlanFLN 60×/1.25. To improve signal-to-noise ratio, images were deconvolved using the Huygens Scripting software (Scientific Volume Imaging) and the algorithm based on the Classic Maximum Likelihood estimator. Images were analyzed using ImageJ (National Institutes of Health).

ACKNOWLEDGMENTS. We thank Dr. F. Zhou, B. Zhang, Dr. J. Twiss, Dr. A. Pacheco, Dr. J. Valenzuela, B. de Blasi, J. Gallardo, M. Díaz, and P. Ayala for technical assistance. C.G. was supported by Mejoramiento de la Calidad y la Equidad en la Educación Superior (MECESUP). A.C. was supported by Fondo Nacional de Desarrollo Científico y Tecnológico (FONDECYT) 1140617 and Iniciativa Científica Milenio (ICM) P09-015-F.

1. González C, Couve A (2014) The axonal endoplasmic reticulum and protein trafficking: Cellular bootlegging south of the soma. *Semin Cell Dev Biol* 27:23–31.
2. Hirokawa N, Takemura R (2005) Molecular motors and mechanisms of directional transport in neurons. *Nat Rev Neurosci* 6(3):201–214.
3. Court FA, Alvarez J (2011) Slow axoplasmic transport under scrutiny. *Biol Res* 44(4): 311–321.
4. Donnelly CJ, Fainzilber M, Twiss JL (2010) Subcellular communication through RNA transport and localized protein synthesis. *Traffic* 11(12):1498–1505.
5. Pannese E, Ledda M (1991) Ribosomes in myelinated axons of the rabbit spinal ganglion neurons. *J Submicrosc Cytol Pathol* 23(1):33–38.
6. Zelená J (1972) Ribosomes in myelinated axons of dorsal root ganglia. *Z Zellforsch Mikrosk Anat* 124(2):217–229.
7. Zelená J (1970) Ribosome-like particles in myelinated axons of the rat. *Brain Res* 24(2):359–363.
8. Vuppalanchi D, Willis DE, Twiss JL (2009) Regulation of mRNA transport and translation in axons. *Results Probl Cell Differ* 48:193–224.
9. Koenig E, Adams P (1982) Local protein synthesizing activity in axonal fields regenerating in vitro. *J Neurochem* 39(2):386–400.
10. Van Minnen J, et al. (1997) De novo protein synthesis in isolated axons of identified neurons. *Neuroscience* 80(1):1–7.
11. Yoon BC, Zivraj KH, Holt CE (2009) Local translation and mRNA trafficking in axon pathfinding. *Results Probl Cell Differ* 48:269–288.
12. Campbell DS, Holt CE (2001) Chemotropic responses of retinal growth cones mediated by rapid local protein synthesis and degradation. *Neuron* 32(6):1013–1026.
13. Yao J, Sasaki Y, Wen Z, Bassell GJ, Zheng JQ (2006) An essential role for beta-actin mRNA localization and translation in Ca2+-dependent growth cone guidance. *Nat Neurosci* 9(10):1265–1273.
14. Leung KM, et al. (2006) Asymmetrical beta-actin mRNA translation in growth cones mediates attractive turning to netrin-1. *Nat Neurosci* 9(10):1247–1256.
15. Willis DE, et al. (2007) Extracellular stimuli specifically regulate localized levels of individual neuronal mRNAs. *J Cell Biol* 178(6):965–980.
16. Willis D, et al. (2005) Differential transport and local translation of cytoskeletal, injury-response, and neurodegeneration protein mRNAs in axons. *J Neurosci* 25(4): 778–791.
17. Tsukita S, Ishikawa H (1976) Three-dimensional distribution of smooth endoplasmic reticulum in myelinated axons. *J Electron Microsc (Tokyo)* 25(3):141–149.
18. Broadwell RD, Cataldo AM (1984) The neuronal endoplasmic reticulum: Its cytochemistry and contribution to the endomembrane system. II. Axons and terminals. *J Comp Neurol* 230(2):231–248.
19. Merianda T, Twiss J (2013) Peripheral nerve axons contain machinery for co-translational secretion of axonally-generated proteins. *Neurosci Bull* 29(4):493–500.
20. Merianda TT, et al. (2009) A functional equivalent of endoplasmic reticulum and Golgi in axons for secretion of locally synthesized proteins. *Mol Cell Neurosci* 40(2):128–142.
21. Spencer GE, et al. (2000) Synthesis and functional integration of a neurotransmitter receptor in isolated invertebrate axons. *J Neurobiol* 44(1):72–81.
22. Brittis PA, Lu Q, Flanagan JG (2002) Axonal protein synthesis provides a mechanism for localized regulation at an intermediate target. *Cell* 110(2):223–235.
23. Pedraza L, Huang JK, Colman DR (2001) Organizing principles of the axoglial apparatus. *Neuron* 30(2):335–344.
24. Rasband MN, Trimmer JS (2001) Developmental clustering of ion channels at and near the node of Ranvier. *Dev Biol* 236(1):5–16.
25. Gasser A, et al. (2012) An ankyrinG-binding motif is necessary and sufficient for targeting Nav1.6 sodium channels to axon initial segments and nodes of Ranvier. *J Neurosci* 32(21):7232–7243.
26. Dugandzija-Novaković S, Koszowski AG, Levinson SR, Shrager P (1995) Clustering of Na+ channels and node of Ranvier formation in remyelinating axons. *J Neurosci* 15(1 Pt 2):492–503.
27. Bi X, Corpina RA, Goldberg J (2002) Structure of the Sec23/24-Sar1 pre-budding complex of the COPII vesicle coat. *Nature* 419(6904):271–277.
28. Sáenz JB, et al. (2009) Golgicide A reveals essential roles for GBF1 in Golgi assembly and function. *Nat Chem Biol* 5(3):157–165.
29. Fujiwara T, Oda K, Yokota S, Takatsuki A, Ikehara Y (1988) Brefeldin A causes disassembly of the Golgi complex and accumulation of secretory proteins in the endoplasmic reticulum. *J Biol Chem* 263(34):18545–18552.
30. Gumy LF, et al. (2011) Transcriptome analysis of embryonic and adult sensory axons reveals changes in mRNA repertoire localization. *RNA* 17(1):85–98.
31. Luo S, et al. (2014) The sodium channel isoform transition at developing nodes of Ranvier in the peripheral nervous system: Dependence on a Genetic program and myelination-induced cluster formation. *J Comp Neurol* 522(18):4057–4073.
32. Boiko T, et al. (2001) Compact myelin dictates the differential targeting of two sodium channel isoforms in the same axon. *Neuron* 30(1):91–104.
33. Al-Bassam S, Xu M, Wandless TJ, Arnold DB (2012) Differential trafficking of transport vesicles contributes to the localization of dendritic proteins. *Cell Reports* 2(1):89–100.
34. Schmidt JW, Catterall WA (1986) Biosynthesis and processing of the alpha subunit of the voltage-sensitive sodium channel in rat brain neurons. *Cell* 46(3):437–444.
35. Aridor M, Fish KN (2009) Selective targeting of ER exit sites supports axon development. *Traffic* 10(11):1669–1684.
36. Sekine S, Miura M, Chihara T (2009) Organelles in developing neurons: Essential regulators of neuronal morphogenesis and function. *Int J Dev Biol* 53(1):19–27.
37. Qu Y, et al. (2001) Differential modulation of sodium channel gating and persistent sodium currents by the beta1, beta2, and beta3 subunits. *Mol Cell Neurosci* 18(5):570–580.
38. Rios JC, et al. (2003) Paranodal interactions regulate expression of sodium channel subtypes and provide a diffusion barrier for the node of Ranvier. *J Neurosci* 23(18):7001–7011.
39. Court FA, Hendriks WT, MacGillavry HD, Alvarez J, van Minnen J (2008) Schwann cell to axon transfer of ribosomes: Toward a novel understanding of the role of glia in the nervous system. *J Neurosci* 28(43):11024–11029.
40. Zhang Y, et al. (2012) Assembly and maintenance of nodes of ranvier rely on distinct sources of proteins and targeting mechanisms. *Neuron* 73(1):92–107.
41. Su YY, et al. (2013) KIF5B promotes the forward transport and axonal function of the voltage-gated sodium channel Nav1.8. *J Neurosci* 33(45):17884–17896.
42. Zurek N, Sparks L, Voeltz G (2011) Reticulon short hairpin transmembrane domains are used to shape ER tubules. *Traffic* 12(1):28–41.
43. Saijilafu HE, Hur EM, Zhou FQ (2011) Genetic dissection of axon regeneration via in vivo electroporation of adult mouse sensory neurons. *Nat Commun* 2:543.
44. Hall A (2006) Rodent sensory neuron culture and analysis. *Curr Protoc Neurosci* Chap 3:Unit 3.19.
45. Twiss JL, Smith DS, Chang B, Shooter EM (2000) Translational control of ribosomal protein L4 mRNA is required for rapid neurite regeneration. *Neurobiol Dis* 7(4):416–428.
46. Zheng JQ, et al. (2001) A functional role for intra-axonal protein synthesis during axonal regeneration from adult sensory neurons. *J Neurosci* 21(23):9291–9303.
47. Sherman DL, et al. (2005) Neurofascins are required to establish axonal domains for saltatory conduction. *Neuron* 48(5):737–742.
48. Ramírez OA, et al. (2009) Dendritic assembly of heteromeric gamma-aminobutyric acid type B receptor subunits in hippocampal neurons. *J Biol Chem* 284(19): 13077–13085.